ORIGINAL ARTICLE

Hob performance degradation assessment method based on cyclic statistical energy

Feiyun Cong[1] · Jiani Wu[1] · Li Chen[1] · Feng Lin[1] · Faxiang Xie[2]

Abstract

During the gear hobbing machine process, the hob performance degradation assessment is significant for optimizing the tool changing frequency and improving machining efficiency. It is challenging to recognize hob wear state through vibration analysis and signal processing. Especially in the condition of intense vibration and noise interference, extracting signal features that reflect the wear state is challenging work. This paper proposes a feature extraction method called Cyclic Statistical Energy (CSE) to obtain the hob wear characteristics by tracking the sensitive frequency band. For the method, the vibration signal model of hob spindle is established first based on the vibration-generation mechanism of the machining process. Then, an index E is proposed to track the wear resonance frequency band of the vibration signal. Furthermore, the cyclic statistical order is analyzed and discussed. The hob performance degradation assessment can be realized by analyzing the energy index E with time variation. The experimental setup has been designed, and the two tests have been conducted in the production line: (1) impact hammer test and (2) hob whole life cutting test. The impact hammer test is set to obtain the modal parameters of the hob. Based on this, the whole life cutting test is designed and realized by which the vibration data of whole life with different wear states can be acquired. The proposed method CSE is successfully applied into online industry experiments test. The results show that the proposed method can give a more accurate performance degradation assessment curve for tool condition monitoring compared with traditional methods such as Wavelet Packet Decomposition (WPD).

Keywords Performance degradation assessment · Signal modeling · Hob · Whole life analysis · Wear state

1 Introduction

Tool is one of the most important and most commonly used elements in the industrial machining process. The tool wear state has a significant influence on the quality of the finished workpiece. By monitoring tool wear conditions in real time, changing tools in advance can be realized [1]. It is beneficial to reduce maintenance costs and improve machining processing efficiency [2]. Therefore, it is necessary to study how to accurately recognize the tool wear state. By now, the tool condition monitoring method has been studied by many scholars.

Vibration signal is one of the common signals and it can be used to continuously monitor the machining process. In terms of vibration signal modeling, Zhou et al. [3] studied the dynamic characteristics of hob spindle by establishing the vibration balance equation of hob spindle and derived the calculation formulas of the vibration displacement in different directions.

Various approaches have been proposed for Tool Condition Monitoring (TCM) by numerous researchers in the past years. Bukkapatnam et al. [4] established a recurrent neural network based on chaos theory and neural networks for flank wear estimation. More importantly, it provides a new direction for future research in degradation assessment. Zhu et al. [5] analyzed the machining sensor signals using WPD for TCM. The result showed that the Root Mean Square (RMS) value is related to the tool wear. They extracted some energy values related to tool wear states for each frequency band and took them as input vectors for the tool state classification. Li et al. [6] proposed a v-support vector regression (v-SVR)-based model for monitoring tool wear. The result

✉ Feiyun Cong
  fycong@zju.edu.cn

1   State Key Laboratory of Fluid Power & Mechatronic Systems, Zhejiang University, Hangzhou, Zhejiang, China

2   Zhejiang Shuanghuan Driveline Co., Ltd, Hangzhou, Zhejiang, China

has shown that the proposed method has a higher predicted accuracy reaching up to 96.76%. Zhu et al. [7] developed an improved hidden semi-Markov Model (HSMM) based on cutting force signals with dependent durations, leading to higher accuracy of tool wear monitoring model in high speed milling. Zhou et al. [8, 9] employed machine learning to realize TCM of milling process. The experimental results both showed an effectively monitoring result. Acoustic signals and cutting force signals were analyzed respectively. In [8], a two-layer angle kernel extreme learning (TAKELM) modal was constructed. The predicted results of wear values are almost consistent with the actual. In [9], a multi-scale edge-labeling graph neural network is proposed with small samples analysis, which can solve the problem of sample insufficiency. Zhu et al. [10] combined numerical simulation and a Generative Adversarial network (GAN) to obtain a large dataset. Then, the dataset is sent to AI classifiers. And the results presented strong classification performance.

In this paper, acceleration signal is selected as the monitored signal. Because of continuous cutting on workpiece in the machining process, the vibration signal energy generated by impact gradually increases with the tool wear increases. Therefore, the vibration signal is highly sensitive to tool wear conditions [11]. While in the present study of tool wear assessment method, internal relations and change rules between vibration signals and tool wear state is not described clearly. In this paper, a hob performance degradation assessment method based on CSE will be investigated on the foundation of theoretical model and experiments.

This paper has been organized in the following way. Section 1 presents the relevant work. The methods used for TCM are reviewed. Section 2 exhibits the hob spindle vibration signal model, which is based on the vibration response model and the periodic impulse model. In Section 3, the CSE is proposed and the order of cyclic statical is discussed. In Section 4, the impact hammer test and hob whole life cutting test is carried out to acquire the acceleration signals. And then, an analysis of data using CSE and WPD is performed to validate the effectiveness of the proposed method. Finally, conclusions are put forward in the final section.

2 Modeling of hob spindle vibration signal

The hob spindle vibration signal model provides a theoretical basis for the study of hob performance degradation assessment. Therefore, the accuracy of the model has a significant impact on the effectiveness of the assessment method. The mechanical vibration of the hob is mainly caused by the hobbing process. During operation, the cutting tool rotates continuously and rapidly with the spindle. The hob meshes with the workpiece to generate a gear tooth profile. Figures 1 and 2 show the diagram of the gear
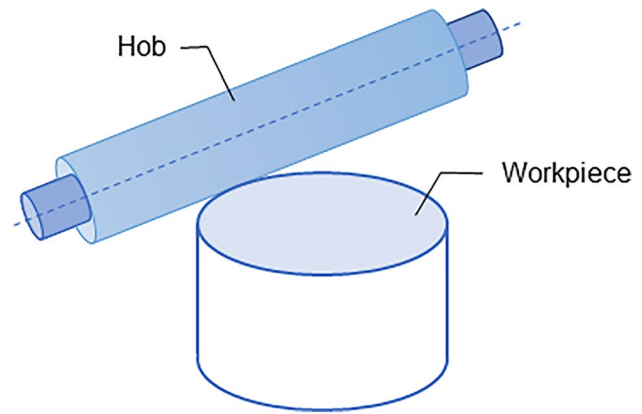

Fig. 1 Diagram of gear hobbing process

Fig. 2 Schematic diagram of gear hobbing impact

hobbing process. The periodic impulse is produced by the relative movement between tool and workpiece. At the time of contact, the impact is generated. When the cutting force act on the tool leads to vibration at its natural frequency, the resonant vibration occurs, and the amplitude of vibration response increases significantly [11]. The signal is analyzed and processed to recognize the hob wear state. Therefore, the hob spindle vibration signal model is established in this section based on the vibration response model and periodic impulse model.

There are some pre-conditions before modeling:

1) The hob is set on a rigid shaft. The machining process is considered an ideal cutting process. The hob with a

rigid shaft has a first critical speed that is higher than the operating speed. The effect of shaft deformation on vibration can be neglected in working condition.

2) It is assumed that the tool is well lubricated. The machining process leads to an increase in temperature caused by friction. The lubrication system can limit the temperature rise and reduce wear and tear. It can meet the heat dissipation requirement so that friction has a little effect on vibration.

3) The mass of the hob can be ignored in the signal model. In the proposed signal model, the mass of the rotor system is not taken into consideration.

4) It is assumed that the motor's output power is constant, and it is sufficient to undertake the maximum load of the working process. The speed of the hob is constant. The influence of drive motor characteristics on the vibration is neglected.

5) The effect of shaft bending deformation and axial deformation on the vibration is neglected.

2.1 Vibration response model of hob spindle system

According to the structure of the hob, a hob can be simplified to a simply supported beam. A series of impulses can be used to simulate the periodic cutting force. Figure 3 shows a simplified schematic of the dynamic model of the hob. In Fig. 3, a three-dimensional coordinate system is established. Its origin is set on one of the pivot points of the beam. The Y_s-axis coincides with the hob axis. The Z_w-axis and X_w-axis are along the radial of the hob.

As shown in Fig. 2, the cutting forces are mainly derived from the relative motion of tool teeth and workpiece. The time interval of force is shown in Fig. 4. A series of transient loads can be expressed by the following equation mathematically, namely the Dirac comb function:

$$\delta(t) = \begin{cases} 1, t = kT_0(k = 0, 1, 2, \dots) \\ 0, \text{else} \end{cases} \qquad (1)$$

where $\delta(t)$ is the impulse series symbol; T_0 is the period of an impulse, and it is related to the hobbing mesh frequency. Because the sudden force acts for an infinitely short
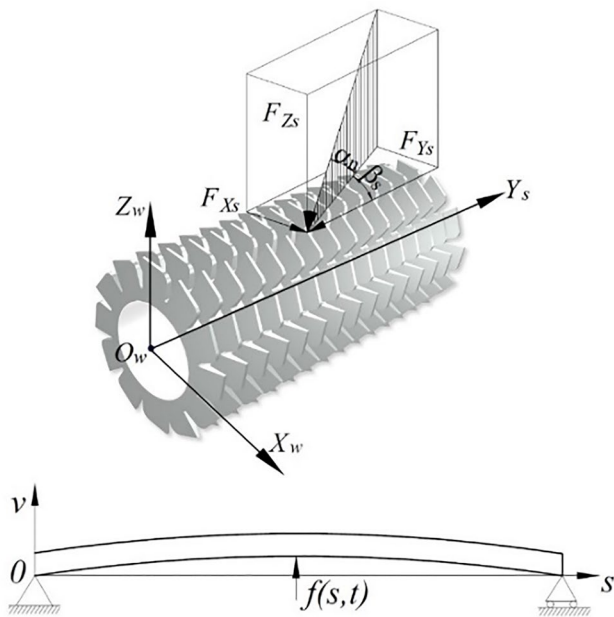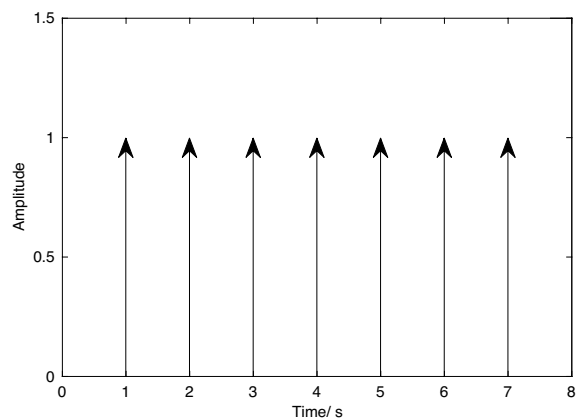

Fig. 3 Dynamic model of hob

Fig. 4 Schematic diagram of unit impulse

time, the hob vibration can be regarded as a weakly damped oscillation.

According to Newton's Second Law of Motion, the differential equation of motion for hob spindle during the dynamic hobbing process can be established as Eq. (2) [12]:

$$m\ddot{h} + c\dot{h} + kh = \delta(t) \tag{2}$$

where m, c, and k represent the equivalent mass, damping coefficient, and stiffness factor of the hob. h is the vibration displacement; $\delta(t)$ is the transient cutting force of gear hobbing, that is, the Dirac comb function.

The detailed procedure for solving Eq. (2) is listed as follows:

Set $c/m = 2n, k/m = (2\pi f_n)^2 = \omega_n{}^2$, Eq. (2) is equivalent to Eq. (3):

$$\ddot{h} + 2n\dot{h} + (2\pi f_n)^2 h = \frac{1}{m}\delta(t) \tag{3}$$

where ωn is known as the natural angular frequency of the system, which is in the unit of rad/s. It also can be called the natural frequency or the resonance frequency. Moreover. ωn is related to the parameters of the system only, such as m and k, not to the initial conditions. f_n is the intrinsic frequency of the system, which is in the unit of Hz.

When the system is free of impulsive force, i.e., $\delta(t) = 0$, the equation above becomes:

$$\ddot{h} + 2n\dot{h} + (2\pi f_n)^2 h = 0 \tag{4}$$

Equation (4) is a second-order, linear differential equation. Set its solution as $h = Ae^{st}$ and substitute the solution into Eq. (4). The characteristic equation can be obtained:

$$s^2 + 2ns + (2\pi f_n)^2 = 0 \tag{5}$$

The characteristic root of Eq. (5) is solved as:

$$s = -n \pm \sqrt{n^2 - (2\pi f_n)^2} \tag{6}$$

In the underdamped case, $n < \omega n$. Thus, the two roots of s can be expressed as:

$$s_{1,2} = -n \pm j\sqrt{(2\pi f_n)^2 - n^2} = -n \pm j(2\pi f_d) \tag{7}$$

in Eq. (7),

$$j = \sqrt{-1}, f_d = f_n\sqrt{1 - \xi^2}, \xi = \frac{c}{2\sqrt{mk}} \tag{8}$$

where f_d is called the damped natural frequency, which is in the unit of Hz. ξ is the damping ratio of the system. The solution for Eq. (4) is:

$$h = e^{-nt}(C_1 e^{j2\pi f_d t} + C_2 e^{-j2\pi f_d t}) \tag{9}$$

According to Euler's formula,

$$\sin(2\pi f_d t) = \frac{1}{2j}(e^{j2\pi f_d t} - e^{-j2\pi f_d t}) \tag{10}$$

$$\cos(2\pi f_d t) = \frac{1}{2}(e^{j2\pi f_d t} + e^{-j2\pi f_d t}) \tag{11}$$

Equation (9) can be written as:

$$h = e^{-nt}(C_3\cos(2\pi f_d t) + C_4\sin(2\pi f_d t)) \tag{12}$$

or

$$h = Ae^{-nt}\sin(2\pi f_d t + \varphi_1) \tag{13}$$

At the moment of sudden force action ($t = t_0 \rightarrow t_0{}^+$), the acceleration is $\ddot{h}_0 = \frac{1}{m}\delta(t)$. The velocity $\dot{h}_0$ and displacement h_0 after the impulse can be calculated as follows:

$$\dot{h}_0 = \int_{t_0}^{t_0{}^+}\ddot{h}dt = \int_{t_0}^{t_0{}^+}\frac{1}{m}\delta(t)dt = \frac{1}{m} \tag{14}$$

$$h_0 = \int_{t_0}^{t_0{}^+}\dot{h}dt = \int_{t_0}^{t_0{}^+}\frac{1}{m}dt = 0 \tag{15}$$

Substitute Eq. (14) and Eq. (15) into the previous equation, and the solution can be expressed as:

$$A_0 = \frac{1}{m2\pi f_d} \tag{16}$$

$$h(t) = A_0 e^{-nt}\sin(2\pi f_d t + \varphi_2) \tag{17}$$

or

$$h(t) = \frac{1}{m2\pi f_n\sqrt{1 - \xi^2}}e^{-\xi 2\pi f_n t}\sin(2\pi f_n\sqrt{1 - \xi^2}t + \varphi_2) \tag{18}$$

Equation (18) is called the unit impulse response function, which is a quasi-periodic function.

The unit impulse response curve of the hob is shown in Fig. 5. It can be seen that the weak damping free vibration is a reduced amplitude reciprocating motion rather than a strictly periodic vibration. It is called quasi-periodic vibration. The period of oscillation is:

$$T_d = \frac{1}{f_d} = \frac{1}{f_n\sqrt{1 - \xi^2}} \tag{19}$$

2.2 Periodic impulse model

The value of cutting force in gear machining is related to tool material, machining parameters, geometric dimensioning, etc. [13]. It can be calculated as Eq. (20), which is an
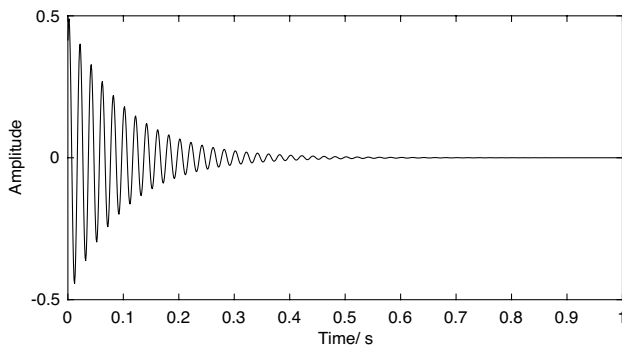
Fig. 5 Unit impulse response curve

empirical formula obtained from a large number of tests [14].

$$Q = \frac{2000M_n{}^{0.95}S_a{}^{0.8}T^{0.15}e^{0.012\beta}C_g}{V^{0.28}i^{0.7}B^{0.6}}e^{0.65XZ^{-0.35}}C_W \times 9.8(\mathrm{N}) \tag{20}$$
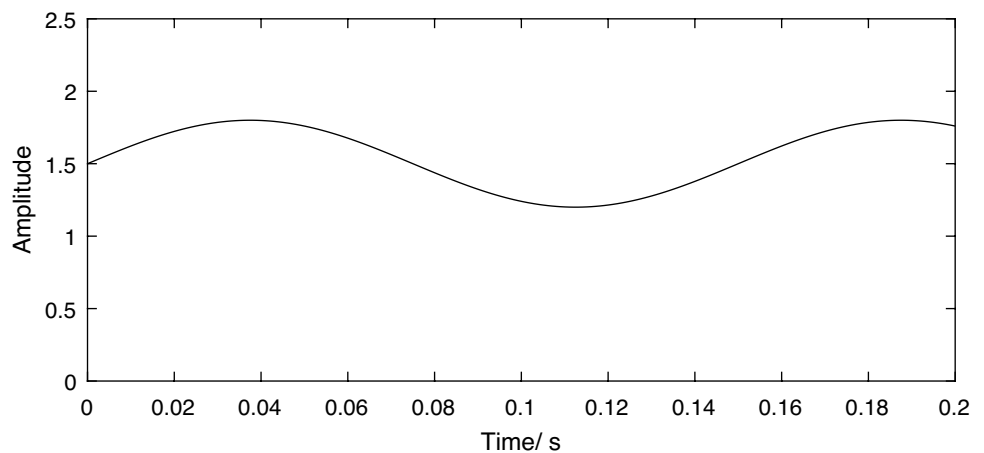
where M_n is the normal module (mm); S_a is the axial feed rate (mm/r); T is the cutting depth (mm) ($T = t/2.25M_n$, t is the feed depth.); V is the cutting speed (m/min); i is the number of hob grooves; C_w is the workpiece material coefficient; B is the hob coefficient ($B = R/M_n$, R is the hob radius.); X is the tooth shape correction factor; Z is the number of the workpiece teeth; β is the helix angle; C_g is the coefficient of the hob threads number.

The mass eccentricity of hob is common in the gear hobbing process. It is mainly caused by misalignment, dimension error of machining, hob wear degree, and so on. It has an influence on the cutting force. The cutting force is not a constant value. It can be expressed as follows:

$$Q' = Q(1 + \lambda\cos(2\pi f_r t + \varphi_3) \tag{21}$$

where f_r is the hobbing frequency; λ is the volatility factor.

In the hobbing process, the load applied to the hob is mainly from the cutting force. The cutting force in Z direction can be expressed as:

$$Q_z = Q'\sin\alpha_n \tag{22}$$

where α_n is the nominal pressure angle.

Therefore, the force applied to hob in Z direction can be expressed as Eq. (23). It is shown in Fig. 6.

$$A(t) = Q\sin\alpha_n(1 + \lambda\cos(2\pi f_r t + \varphi_3)) \tag{23}$$

The periodic impulse can be derived by multiplying the unit impulse $\delta(t)$ and the cutting force in Z direction $A(t)$, as shown in Fig. 7:
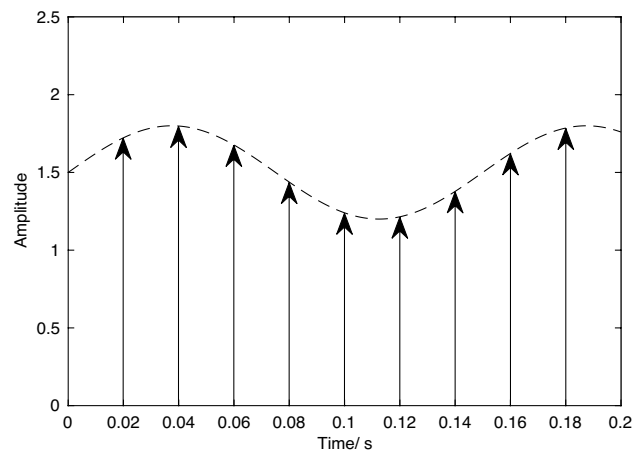
$$f(t) = A(t) \cdot \delta(t) \tag{24}$$

Fig. 7 Schematic diagram of periodic impulse

Fig. 6 Schematic diagram of the load of hob in Z direction

2.3 Hob spindle vibration signal model

The vibration signal of hob spindle is modeled as the superposition of repetitive damped oscillation signals. The convolution of the two models presented above can be used to express the hob spindle vibration signal. The expression is listed as follows [15]:

$$x(t) = [A(t) \cdot \delta(t)] * h(t) = \int_{-\infty}^{+\infty} [A(t) \cdot \delta(t)]h(t - \tau)d\tau \tag{25}$$

where symbol "*" denotes the convolution operation. Then, substitute Eqs. (1), (23), and (24) into Eq. (25). The calculated expression for the hob vibration signal can be obtained as follows:

$$\begin{aligned} x(t) &= [Qsin\alpha_n + F_m cos(2\pi f_r t + \varphi_3)] \cdot \delta(t) * h(t) \\ &= \int_{-\infty}^{+\infty} [Qsin\alpha_n + F_m cos(2\pi f_r t + \varphi_3)] \cdot \delta(t)h(t - \tau)d\tau \end{aligned} \tag{26}$$

By combining the above derivation process, the simulated signal model of hob spindle can be obtained as follows:

$$\begin{cases} x(t) = \sum_{i=1}^{N} A(t) \cdot h(t - iT_0 - \tau_i) + n(t) \\ A(t) = Qsin\alpha_n (1 + \lambda cos(2\pi f_r t + \varphi_3)) \\ h(t) = A_0 e^{-\xi 2\pi f_n t} sin(2\pi f_d t + \varphi_2) \end{cases} \tag{27}$$

In this equation, $x(t)$ is the analog vibration signal shown in Fig. 8; $h(t)$ is the unit impulse response model; $n(t)$ is the fixed noise signal; $A(t)$ is the impact amplitude; T_0 is the minimum pulse period. τ_i is the slight fluctuation of the ith impact relative to the mean period T_0.

The following are some points about the simulated signal to be discussed:

1) As shown in Fig. 8, the hob vibration signal is nonlinear and nonstationary. It displays an apparent periodic alternating variation because of the interrupted cutting process.

2) A single impulse response represents a single collision between hob tooth and gear.
3) The middle of two peaks contains two parts. One is the impulse response caused by impact. The other one is forced vibration, which is caused by the continuous hobbing excitation.
4) The interval between two pulses represents the time interval between two adjacent hob teeth and workpiece, which is related to the speed and number of hob grooves. It can be calculated as follows:

$$f = \frac{n_h \times i}{60} \tag{28}$$

where n_h is the spindle rotational speed in unit of rpm.

3 Cyclic Statistical Energy (CSE) method

The Root Mean Square (RMS) value is usually applied for condition monitoring of rotating machines, which can reflect the energy and amplitude of a monitored signal in the time domain [16]. Nevertheless, it is not sensitive enough for early wear [17]. In the TCM tests, the spectrum of the acquired signals differs when the tool is in different wear states. Therefore, processing signals in frequency domain is helpful for tool wear state recognition. An increase in hob wear causes worse surface roughness and accuracy of the workpiece. The energy of the vibration signals gradually increases with the hob wear increase as well [18]. Therefore, the CSE is proposed based on impact energy.

Fig. 8 Vibration simulation signal of hob spindle
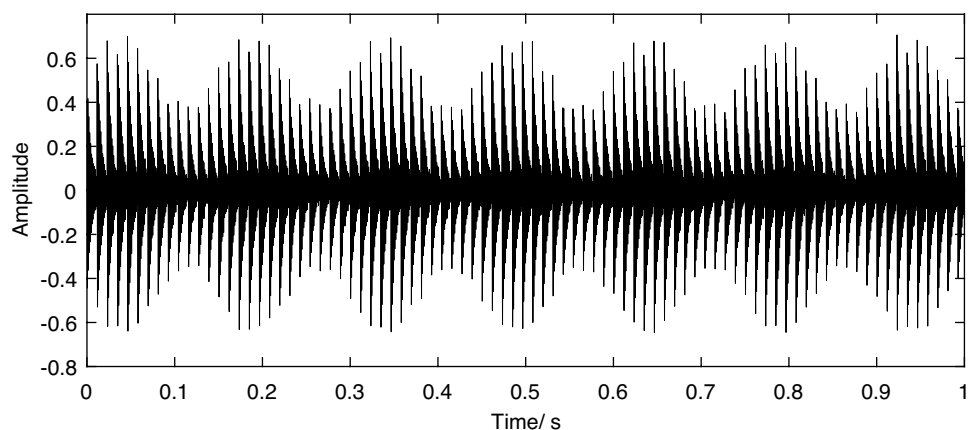
3.1 Performance degradation method based on cyclic statistical energy sequence

3.1.1 Discrete Fourier transform (DFT)

Spectral analysis is widely used in engineering testing, such as gear machine fault diagnosis, sensor signals denoising, etc. Its essence is to transform the waveform of the signal in the time domain into the frequency spectrum in the frequency domain, so as to quantitatively explain the information of the signal. Fourier transform is a spectral analysis method to decompose a time domain signal and expand it by frequency, making it a function in frequency. In this way, the signal can be studied and analyzed in frequency domain. The Fourier transform is shown in Eq. (29) and the inverse Fourier transform is shown in Eq. (30).

$$F(\omega) = \int_{-\infty}^{+\infty} f(t)e^{-j\omega t}dt \tag{29}$$

$$f(t) = \frac{1}{2\pi}\int_{-\infty}^{+\infty} F(\omega)e^{-j\omega t}d\omega \tag{30}$$

where $F(\omega)$ is a continuous spectral function of $f(t)$ and generally, it is a complex function that can be written as: $F(\omega) = |F(\omega)|e^{-j\varphi(\omega)}$; $f(t)$ is a time-domain non-periodic signal; ω is the angular frequency.

Since the acquisition equipment has a sampling period, the acquired signals are discrete. Also, there is a fast and effective algorithm for calculating discrete Fourier. Therefore, discrete Fourier transform (DFT) plays a central role in various digital signal processing algorithms. It has a wide range of applications in signal processing. The DFT is the Fourier transform discretized in the frequency domain. The DFT is defined as Eq. (31), and the inverse discrete Fourier transform is defined as Eq. (32):

$$X(k) = \sum_{n=0}^{N-1} x(n)e^{-\frac{2j\pi kn}{N}} (k = 0, 1, 2, \ldots, N-1) \tag{31}$$

$$x(n) = \frac{1}{N}\sum_{k=0}^{N-1} X(k)e^{-\frac{2j\pi kn}{N}} (n = 0, 1, 2, \ldots, N-1) \tag{32}$$

In this equation, N is the number of samples; n is the sequence number of discrete values in the time domain; k is the sequence number of discrete values in the frequency domain.

Set x_n as a discrete-time signal of N samples long. The discrete Fourier transform is performed on x_n that is acquired during the monitoring test. The complex signal s_k can be calculated as follows:

$$s_k = \sum_{n=1}^{N} x_n e^{-\frac{2j\pi kn}{N}} (k = 1, \ldots, N) \tag{33}$$

3.1.2 Short time interception

Analysis of the intercepted short sequence segment of signals can improve the identification of partial features. Set the cyclic statistical order n as the length of the subsequence. The discrete sequence s_k is intercepted by slipping. Thus, the cyclic statistical sequence can be acquired:

$$y_i = s_i, s_{i+1}, s_{i+2}, \ldots, s_{i+n-1} \tag{34}$$

where y_i is the discrete subsequence obtained by the ith slip interception.

3.1.3 Obtain the index E

From the above sequence, a circular statistical matrix can be defined as follows:

$$V = \begin{bmatrix} y_1 \\ \cdots \\ y_{i+1} \\ \cdots \\ y_{N-n+1} \end{bmatrix} = \begin{bmatrix} s_1 & s_2 & \cdots & s_{n-1} & s_n \\ \cdots & \cdots & \cdots & \cdots & \cdots \\ s_{i+1} & s_{i+2} & \cdots & s_{i+n-1} & s_{i+n} \\ \cdots & \cdots & \cdots & \cdots & \cdots \\ s_{N-n+1} & s_{N-n+2} & \cdots & s_{N-1} & s_N \end{bmatrix} \tag{35}$$

The circular statistical energy matrix (CSEM) can be defined as follows:

$$S = V \cdot V^T \tag{36}$$

Extract the main diagonal elements of CSEM obtained from Eq. (36) and construct the cyclic statistical energy sequence R:

$$R_i = S_{ii}(i = 1, 2, 3, \cdots I, I = N - n + 1) \tag{37}$$

R_i is the ith element of the matrix $\mathbf{R}$. S_{ii} is the element of the ith row and the ith column of the matrix $\mathbf{S}$. The optimal cyclic statistical energy sequence is:

$$R_h = \max\{R_i, (i = 1, 2, 3, \cdots I, I = N - n + 1)\} \tag{38}$$

The following equation proposes an index E for assessing the degradation degree of hob performance, based on the optimal cyclic statistical energy sequence:

$$E = \sqrt{\frac{1}{n}\sum_{k=h+1}^{h+n} s_k^2} \tag{39}$$

3.2 Determination of the order of cyclic statistics

With the hob wear increase, the impact will stimulate more high-frequency signals. It is important to track the energy

concentration frequency band because it contains mostly wear information. The CSE is proposed from the perspective of frequency band energy. The tool wear characteristics are quantified by comparing the energy of different vibration signals in the energy concentration frequency band. Therefore, set the bandwidth of the energy concentration band as the cyclic statistical order.

In this paper, the half-power bandwidth method is used to determine the range of the energy concentration band. Firstly, the maximum value $|X(\omega_n)|$ can be easily found in the vibration signal spectrogram. The two half-power frequency points can be calculated as:

$$|X(\omega_1)|=|X(\omega_2)| = \frac{1}{\sqrt{2}}|X(\omega)| \tag{40}$$

Then the expression for the cyclic statistical bandwidth B_w can be written as Eq. (41) by assuming that $\omega_2 > \omega_1$:

$$B_w = \omega_2 - \omega_1 \tag{41}$$

The expression for frequency resolution p is as follows:

$$p = \frac{f_s}{N} \tag{42}$$

where N is the number of samples and f_s is the sampling frequency. An expression for the cyclic statistical order n can be obtained as:

$$n = \frac{B_w}{p} \tag{43}$$

Based on the calculations proposed above, the following points can be made about the order of the cyclic statistics:

1) The order of cyclic statistics is determined by the sampling frequency and the bandwidth of cyclic statistics. The higher the sampling frequency, the smaller the order of cyclic statistics.
2) When the parameter n is too large, it will lead to an increase in computation. Whereas when the parameter n is too small, it may lead to a decrease in recognition accuracy to extract the fault features.

Therefore, a reasonable cyclic statistical order n is the basis for constructing an optimal cyclic statistical energy sequence. It has an important impact on the assessment of the degree of hob performance degradation.

Based on the analysis above, the flow chart of the CSE is shown in Fig. 9.

Fig. 9 The flow chart of CSE
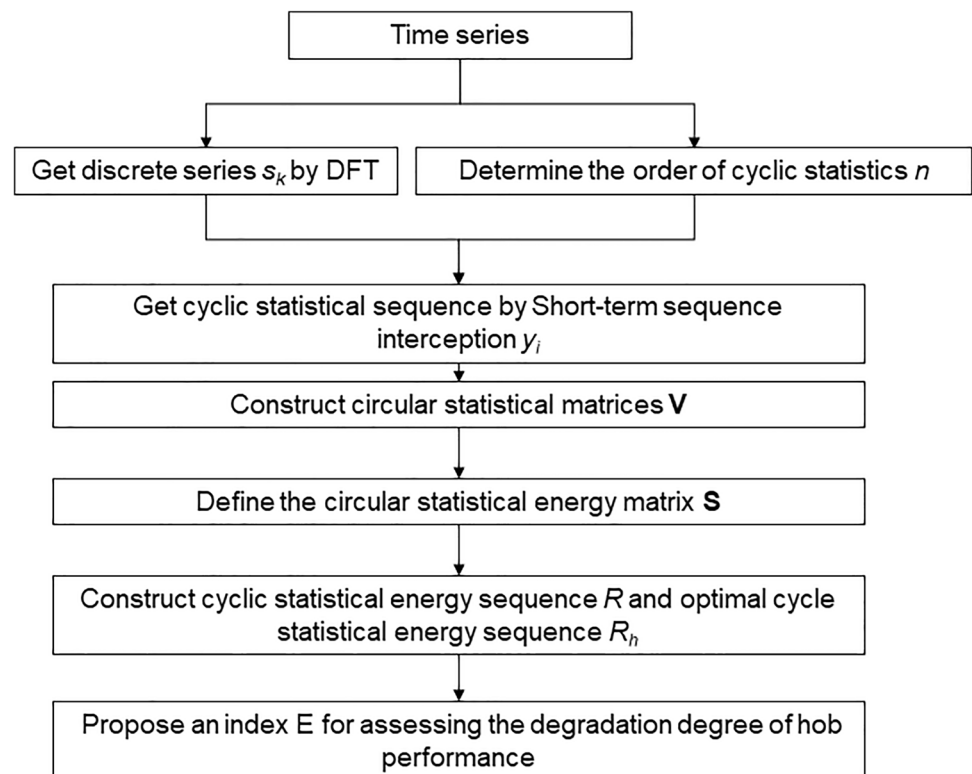
4 Experimental validation and verification

4.1 Experimental setup

To validate the effectiveness of the proposed CSE, the experiment for gear hobbing machining is carried out. The validation experiment consists of two parts: (1) impact hammer test and (2) hob whole life cutting test. Firstly, the modal parameters of the hob spindle can be acquired by the impact hammer test. Thus, the cyclic statistical order n can be determined. Secondly, the cutting vibration signals of a hob in different wear states were acquired in the hob whole life cutting test.

The hobbing test is carried out in a production site for automobile gear manufacturing in Shuanghuan Transmission Stock Company on a CNC machining center YDA313. The picture of equipmental setup is shown in Fig. 10. The workpiece is machined by the hob, and the parameters of machined gear are listed in Table 1. The characteristics of the tool used for two tests are illustrated in Table 2. A modal hammer is used to hit the hob to get the modal parameters, which is shown in Fig. 11. The schematic diagram of the experimental setup is shown in Fig. 12.

In order to monitor the tool condition, the vibration signals are measured by a CA-YD-1182 accelerometer. The accelerometer is mounted on the non-rotating part of hob spindle by magnetic attachment. It is oriented along the Z direction. And the sampling system is set to 12.8 kHz. The


Fig. 10 Experimental equipment. **a** Hob. **b** The experimental platform for hobbing. **c** Data acquisition system. **d** Hobbing machine

Table 1 Geometry of the gear

Part name	Number of gear teeth	Material brand	Dedendum circle diameter (mm)	Common normal line (mm)	Gear module	Helix angle
Counter shaft	17	ZF7B	71.7	48.824	4.5	16.5°

Table 2 Characteristics of the tool

Model number	Number of hob grooves	Outer diameter (mm)	Module	Max speed of rotation (rpm)	Lubricating method
GM58125.II-03–001	11	80	4.5	400 (rough machining)/420 (finish machining)	Dry cutting

Fig. 11 Modal hammer
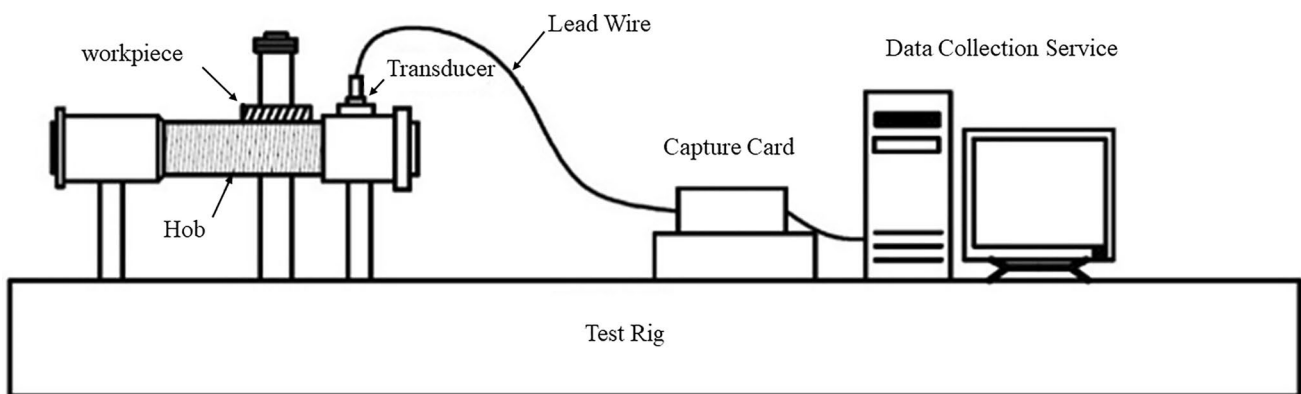
Fig. 12 Schematic diagram of the experimental setup

data acquisition system consists of a data acquisition card, data acquisition software, and a personal computer (PC). The data acquisition card NI-9234 transfers the acceleration signals collected by the sensor to the PC. Then, the collected signals can be displayed in real time and stored stably by the data acquisition software.

4.2 Experiment 1: impact hammer test

4.2.1 Data acquisition

The impact hammer excitation method is adopted to obtain dynamic characteristics of the hob. An impact hammer test is applied on the tool tip in Z direction to measure the modal parameters of the spindle. The hitting point is shown in Fig. 10(a). The impact hammer was applied vertically at the knocking point, and the force is excited by the hammer within a very short time. Then, the response signals generated by impact are obtained by the accelerometer mounted on the hob spindle. The data length is 0.05 s and there are 640 sampling points. The testing signals in the time and frequency domain are shown in Fig. 13(a) and (b), respectively. As can be seen in Fig. 13, the resonant peak is near 1000 Hz, where the energy of the hob vibration signals is concentrated.

4.2.2 Signal analysis

To explore more about the dynamic characteristics of the hob during the gear cutting process, it is necessary to

Fig. 13 Impulse signal. **a** Waveform. **b** Fourier spectrum
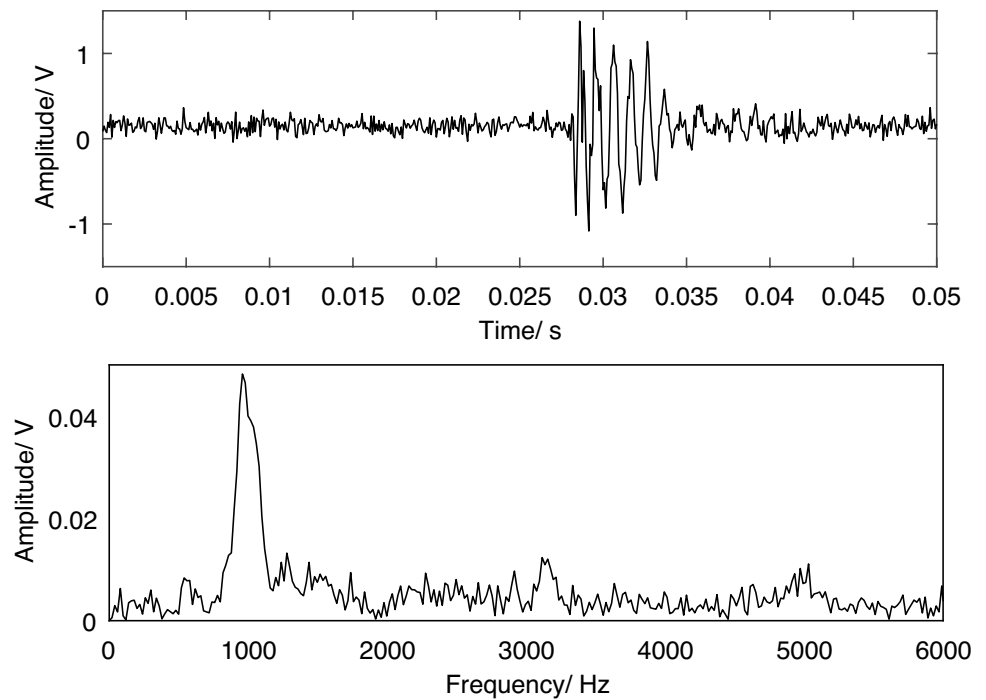
determine the energy concentration frequency band of the vibration signal specifically. The corresponding frequency at half power is about:

$$\omega_1 = 923\text{Hz}; \omega_2 = 1073\text{Hz} \tag{44}$$

The cyclic statistical bandwidth B_w is:

$$B_w = \omega_2 - \omega_1 = 1073 - 923 = 150\text{Hz} \tag{45}$$

The frequency resolution p_1 of modal test vibration signals is:

$$p_1 = \frac{f_s}{N} = \frac{12800}{640} = 20 \tag{46}$$

4.3 Experiment 2: hob whole life cutting test

4.3.1 Data acquisition

A new hob is used for machining to ensure the accuracy of the test. During the whole cutting tool life cycle, 144 gears were machined with the hob. Figure 14 represents microscopic photographs of the gears machined by the bob in the different wear states. It can be seen that the gears accuracy decreases with the hob wear increases. To investigate the development of the wear state, the vibration signals were acquired in the cutting process by the equipment shown in Fig. 10. A set of data was collected for each workpiece. The sampling frequency of the vibration signal is 12.8 kHz. To characterize the hobbing process well, 64000 sampling

points for each set of data in the stable stage is selected as initial data. And the data length is 5 s. The total data length is calculated as: $64000 \times 144 = 9216000$. This information is listed in Table 3.

The collected hob spindle acceleration signals are analyzed with time and frequency domain analysis. Figures 15 and 16 show the vibration time-domain signal and the vibration signal spectrum when the hob is in the state of initial wear, normal wear, and severe wear, respectively.

The hob spindle rotates at a constant rotational speed of 400 rpm. The corresponding rotational frequency can be calculated as: $400 \div 60 = 6.67\text{Hz}$. The number of hob grooves is 13. So the corresponding hob meshing frequency can be found in the frequency domain diagram: $6.67 \times 13 = 86.7\text{Hz}$. And the corresponding cutting time for each tooth in the time domain diagram is: $60 \div (400 \times 13) = 0.0115\text{s}$. It can be seen that the vibration signal consists of a series of distinct impacts in Fig. 15. However, it is difficult to artificially determine the range of energy concentrated frequency band in the time domain.

4.3.2 Results and discussion

To study the relationship between the RMS and hob wear state, the RMS value of collected signals have been calculated for 144 workpieces, which is shown in Fig. 17. There is not a clear trend in the graph. It also can be seen that the vibration of RMS value cannot reflect the hob performance degradation process. Therefore, the CSE is adopted to analysis data.

Fig. 14 Gears machined by hob in different wear states. **a** Initial wear. **b** Normal wear. **c** Severe wear

Table 3 Summary of the collected data

Number of workpiece	Sampling frequency	Collected data length of each gear	Total data length
144	12.8 kHz	64000	9216000

To improve computational efficiency, a segment of data is intercepted with a guaranteed frequency resolution. The intercepted data length is 2 s and the sampling points of each group is 25600. The cyclic statistical bandwidth B_w is calculated by (45) and the B_w is 150 Hz. The frequency resolution p_2 of hob whole life cutting test vibration signals is:

Fig. 15 Vibration time domain signal. **a** Initial wear. **b** Normal wear. **c** Severe wear
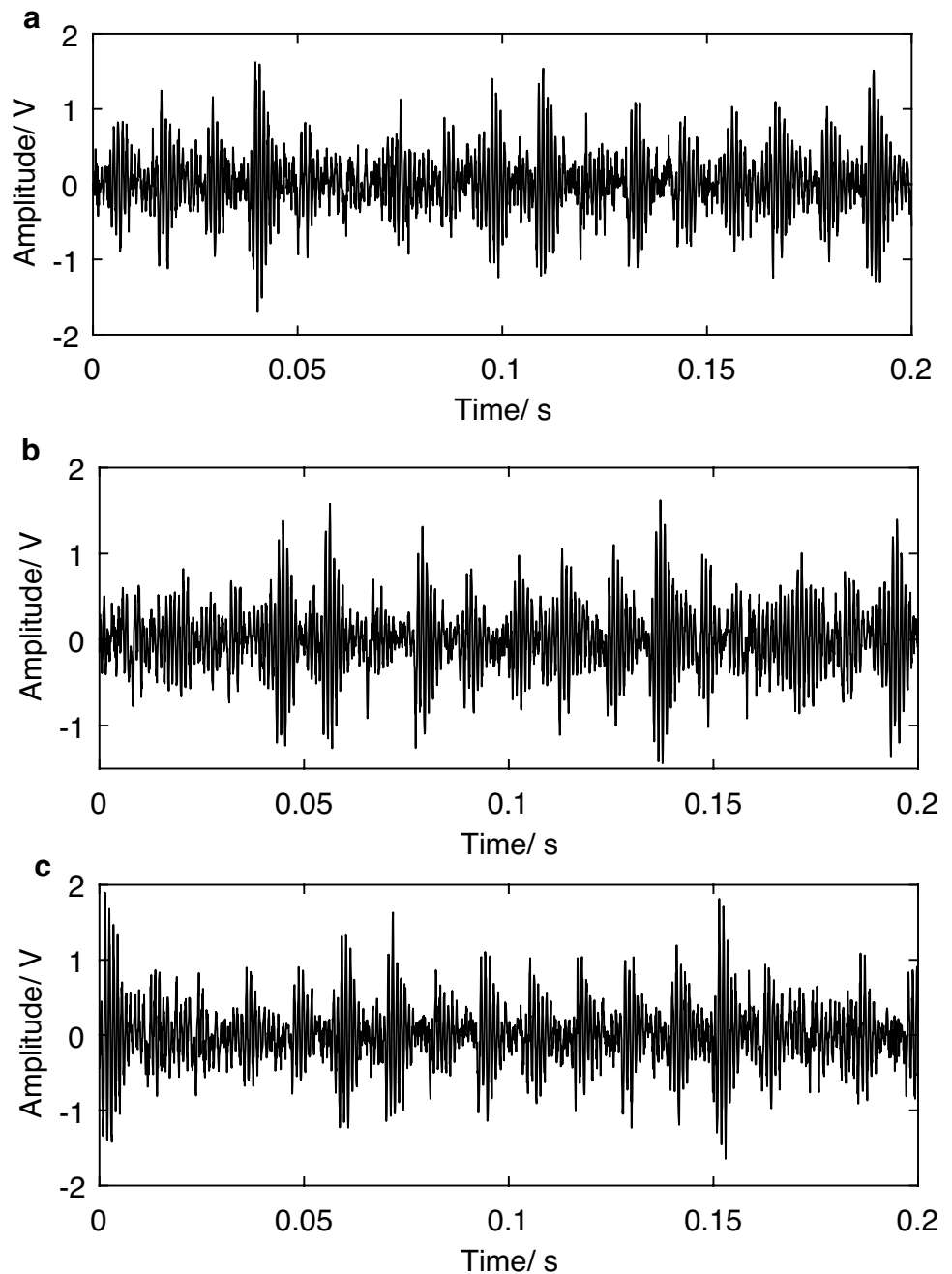
$$p_2 = \frac{f_s}{N} = \frac{12800}{25600} = 0.5 \tag{47}$$

The order n of hob whole life cutting test vibration signals is:

$$n = \frac{B_w}{p_2} = \frac{150}{0.5} = 300 \tag{48}$$

The cyclic statistical energy sequence and the maximum value of sequence are acquired. The corresponding point is shown in Fig. 18. Thus, the optimal cyclic

statistical energy sequence is $\{s_{814}, s_{815}, \ldots, s_{1113}\}$. The optimal cyclic statistical sequence is taken as the calculation sequence for each workpiece, which contains the energy concentration band. The index E is calculated to assess hob performance degradation degree. The Moving Average filter (MAF) is adopted to analyze data points in discrete systems, which can smooth out the short-term fluctuations. Firstly, N consecutive sample points are taken as a queue. And then, the average of N data in the queue is calculated. Place new data at the end of the original queue and discard the data at the start each time. The E sequence

Fig. 16 Vibration signal spectrum. **a** Initial wear. **b** Normal wear. **c** Severe wear
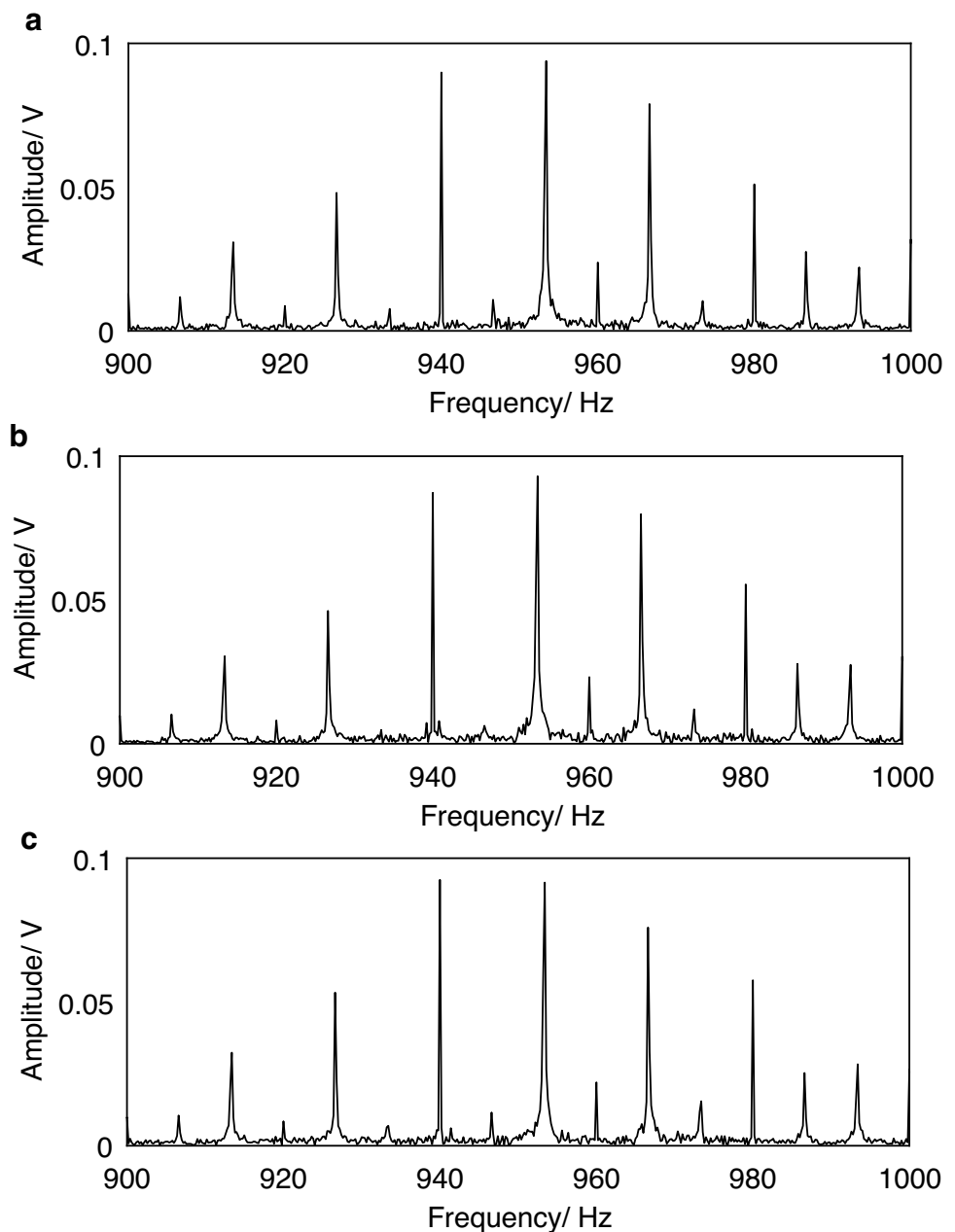
is processed by the MAF method. The result is shown in Fig. 19, showing an increasing tendency.

From the perspective of microscopic mechanism, the tool wear progression can be divided into four stages: (1) coating wear stage (group 0–45): the indicator of degradation E is relatively stationary. It indicates that the hob has a good wear resistance because of the coating. The hob is in the stage with optimal performance. (2) Initial wear stage (group 45–70): the surface roughness of the hob increases, and the contact area between the flank face of the tool and the workpiece is smaller. So that the compressive stress caused by cutting force is getting bigger, and the tool wears faster. As a result, the indicators of degradation E increase

steadily. (3) Normal wear stage (group 70–120): the surface roughness of hob decreases, and the tool's cutting edge is flattened after the initial wear stage. The contact area is getting bigger. The wear degree of the tool grows slowly. As a result, the indicators of degradation E rise slowly. (4) Severe wear stage (group 120–144): after a long period of initial wear and steady wear, there is a sharp increase in wear rate because of the change in surface morphology and fatigue of the surface layer. Eventually, the tool fails.

Additionally, the WPD is also adopted to analyze signals as a comparison (Fig. 20). The total vibration signals energy differently when the hob is in different wear states. Thus, the frequency band energy of hob in different wear state
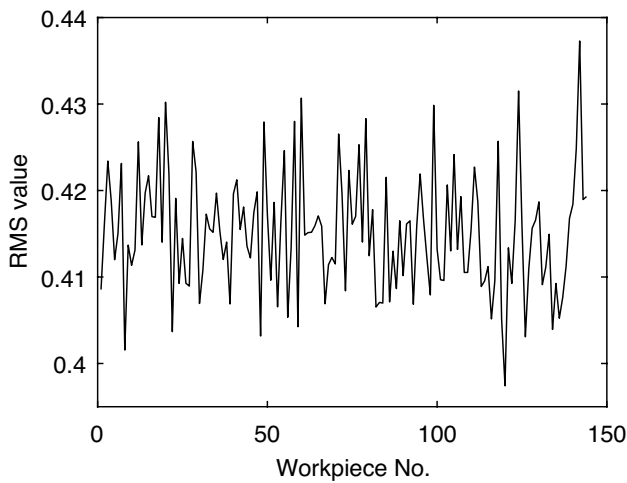
Fig. 17 RMS values of vibration signals for 144 workpiece

Fig. 19 Curve of index *E* obtained by CSE

after WPD also differs. So it can be selected as an index to recognize the hob wear state. A set of acceleration signals is decomposed using wavelet packets. The frequency bandwidth of initial vibration signals is 6400 Hz. The three-layer WPD is applied to process signals. Figure 21 shows the signal analysis results of energy proportion for each frequency band. The diagram shows that energy is concentrated in the second frequency band, and the energy of which is significantly higher than others. The corresponding frequency range is 800–1600 Hz.

The energy in the second frequency band is calculated for all 144 sets of data in the whole life cutting test. As a result, the variation of frequency band energy with the change of hob wear state can be shown in Fig. 20. The comparison of Figs. 19 and 20 results shows that:

1) The *E* values of vibration signals increases with the increase of workpiece number. However, the increasing rate is different when the hob is in different wear states. According to the graph, the variation of *E* is flattening at first and then there is a sharp increase. Later, the increasing rate is flattening again.
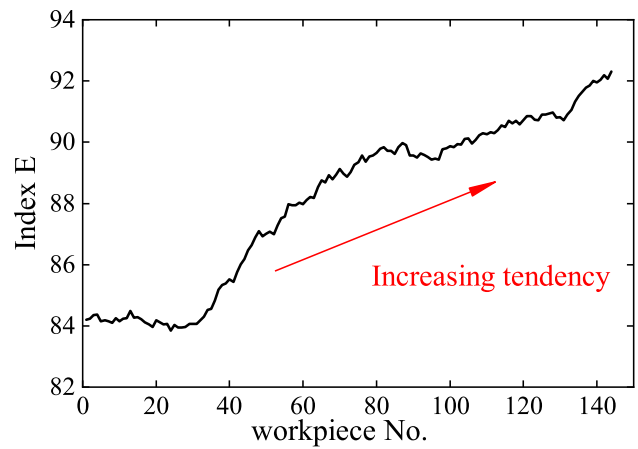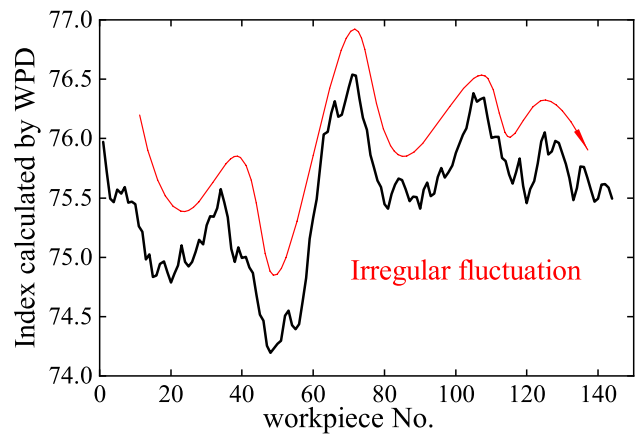

Fig. 20 Curve of index obtained by WPD

2) The variation of indictors obtains by WPD shows an irregular function.

Furthermore, in order to validate the reasonability of the curve in Fig. 19, the workpiece accuracy test is carried out. During the cutting process, the workpiece accuracy

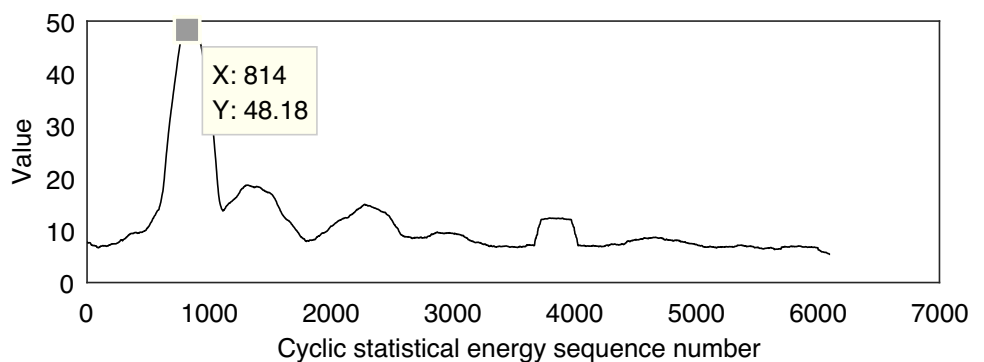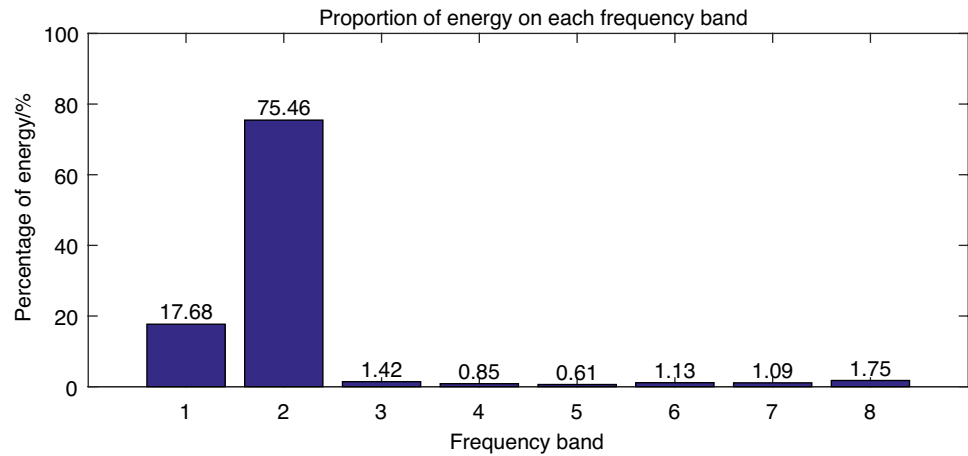**Fig. 18** Cycle statistical energy sequence diagram

Fig. 21 Energy proportion of each frequency band using WPD

decreases and surface roughness increases gradually with tool wear. Therefore, the tool wear state can be reflected by the quality of the workpiece. Two main parameters are given to measure gear quality: tooth profile deviation and total helix deviation. The tooth profile deviation is the normal distance between two designed tooth profiles that enclose the actual working part of the tooth profile, and the distance is the smallest over the evaluation range. The total helix deviation is the distance between two designed helix lines that contain the actual helix traces within the detection range of the probe. In order to verify the effectiveness of the proposed index E, the two indicators of some specific workpieces are measured by the device shown in Fig. 22.

Figure 22(a) shows the initial position of the probe and Fig. 22(b) shows a picture of detection process.

The telescopic probe of testing equipment slides along the surface of a part to record the surface condition. The actual contour line is generated at the display interface simultaneously. The data obtained from the testing equipment is listed in Table 4. Plot the two sets of data as two graphs in Fig. 23(a) and (b).

It has been observed that the tendencies in both plots generally agree with the tendency in Fig. 19(b), while the tendency in Fig. 20 using the WPD is not. The result shows that the proposed performance degradation index E based on CSE has good sensitivity to different wear stages and

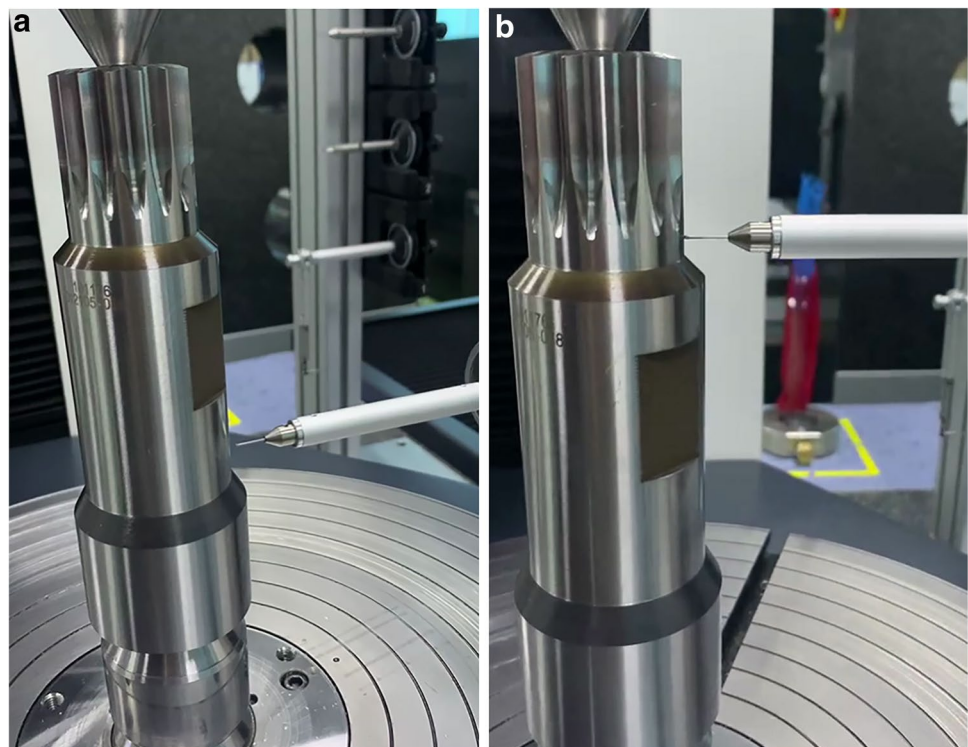**Fig. 22** Picture of test equipment. **a** Initialization. **b** Detection process

Table 4 Total deviation of parts

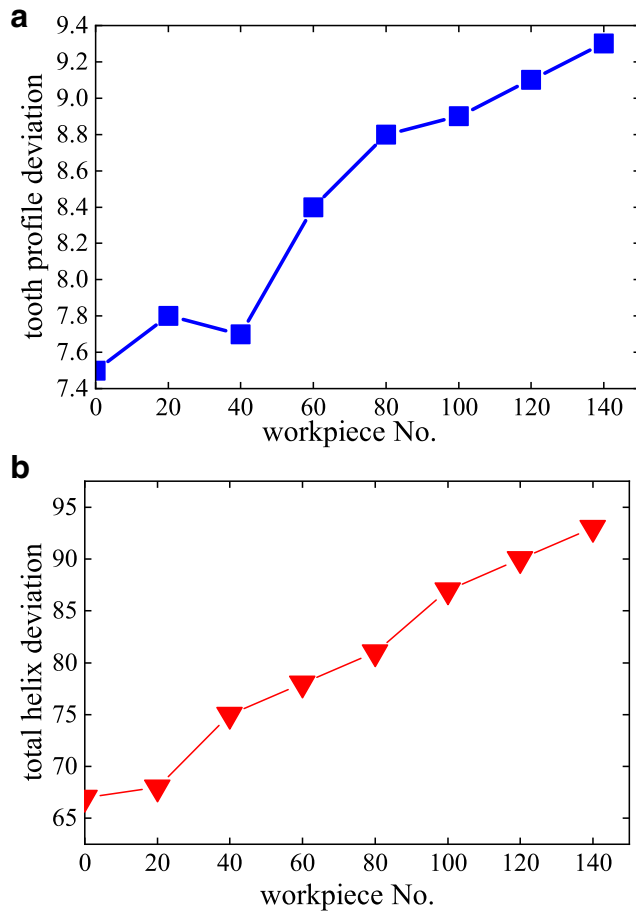| Serial number of parts	0	20	40	60	80	100	120	140
Tooth profile deviation	7.5	7.8	7.7	8.4	8.8	8.9	9.1	9.3
Total helix deviation	67	68	75	78	81	87	90	93

Fig. 23 Trend chart of total deviation of parts. **a** Total deviation of tooth profile. **b** Total deviation of helix

can reasonably reflect the performance degenerate process of the hob.

5 Conclusion

Tool performance degradation assessment is an important part of mechanical machining. In this paper, a new tool wear state recognition method for hobs based on the CSE was proposed. At the beginning of this work, the hob spindle vibration signal model is established to study the dynamic characteristics of hob. The early wear cannot be recognized by the traditional signal analysis approaches, such as RMS and WPD. To solve this problem, the CSE is presented. Firstly, a short time interception is performed on the signals

in frequency domain after DFT. And then the cyclic statistical energy sequence is established by extracting the main diagonal elements of CSEM. The optimal cyclic statistical energy sequence is the max value of the CSEM. The index E is calculated based on the optimal cyclic statistical energy sequence. In order to verify the effectiveness of the CSE, the validation experiments were carried out under industrial circumstances. The analysis results show that the index E is an efficient parameter for recognizing the early wear in hobbing machining compared with WPD.

The CSE shows the superiorities to traditional approaches. It offers a new way for future research not only in hob performance degradation assessment, but also in other rotating machines, such as milling and drilling.

Author contribution Feiyun Cong: conceptualization, supervision, writing—review and editing

Jiani Wu: writing and visualization

Li Chen: methodology, writing, data collection and analysis

Feng Lin: investigation and data curation

Faxiang Xie: resources and data curation

Declarations

Ethics approval The work was original research that has not been published previously and is not under consideration for publication elsewhere, in whole or in part.

Consent to participate Yes, consent to participate from all the authors.

Consent for publication Yes, consent to publish from all the authors.

Conflict of interest The authors declare no competing interests.

References

1. Yu W, Tu W, Kim IY, Mechefske C (2021) A nonlinear-drift-driven Wiener process model for remaining useful life estimation considering three sources of variability. Reliab Eng Syst Saf 212:107631. https://doi.org/10.1016/j.ress.2021.107631

2. Cheng Y, Hu K, Wu J, Zhu H, Shao X (2022) Autoencoder Quasi-Recurrent neural networks for remaining useful life prediction of engineering systems. IEEEASME Trans Mechatron 27:1081–1092. https://doi.org/10.1109/TMECH.2021.3079729

3. Han Z, Ping Y, Pei J, Zhao Z, Luo Q (2020) Research and verification of vibration displacement and acceleration response model

of hob spindle. J Mech Eng 56:72. https://doi.org/10.3901/JME.2020.07.072

4. Bukkapatnam STS, Kumara SRT, Lakhtakia A (2000) Fractal estimation of flank wear in turning. J Dyn Syst Meas Control 122:89–94. https://doi.org/10.1115/1.482446

5. Zhu K, Wong YS, Hong GS (2009) Wavelet analysis of sensor signals for tool condition monitoring: a review and some new results. Int J Mach Tools Manuf 49:537–553. https://doi.org/10.1016/j.ijmachtools.2009.02.003

6. Li N, Chen Y, Kong D, Tan S (2017) Force-based tool condition monitoring for turning process using v-support vector regression. Int J Adv Manuf Technol 91:351–361. https://doi.org/10.1007/s00170-016-9735-5

7. Zhu K, Liu T (2018) Online tool wear monitoring via Hidden Semi-Markov model with dependent durations. IEEE Trans Ind Inform 14:69–78. https://doi.org/10.1109/TII.2017.2723943

8. Zhou Y, Sun B, Sun W, Lei Z (2022) Tool wear condition monitoring based on a two-layer angle kernel extreme learning machine using sound sensor for milling process. J Intell Manuf 33:247–258. https://doi.org/10.1007/s10845-020-01663-1

9. Zhou Y, Zhi G, Chen W, Qian Q, He D, Sun B, Sun W (2022) A new tool wear condition monitoring method based on deep learning under small samples. Measurement 189:110622. https://doi.org/10.1016/j.measurement.2021.110622

10. Zhu Q, Sun B, Zhou Y, Sun W, Xiang J (2021) Sample augmentation for intelligent milling tool wear condition monitoring using numerical simulation and generative adversarial network. IEEE Trans Instrum Meas 70:1–10. https://doi.org/10.1109/TIM.2021.3077995

11. Albertelli P, Braghieri L, Torta M, Monno M (2019) Development of a generalized chatter detection methodology for variable speed machining. Mech Syst Signal Process 123:26–42. https://doi.org/10.1016/j.ymssp.2019.01.002

12. Sivasakthivel P, Sudhakaran R, Rajeswari S (2013) Optimization of machining parameters to minimize vibration amplitude while machining Al 6063 using gray-based Taguchi method. Proc Inst Mech Eng Part B J Eng Manuf 227:1788–1799. https://doi.org/10.1177/0954405413494921

13. Wang S, Yang Y, Zhou J, Li Q, Yang S, Kang L (2011) Effect of machining precision caused by NC gear hobbing deformation. Appl Mech Mater 86:692–695. https://doi.org/10.4028/www.scientific.net/AMM.86.692

14. Yu C, Huang X (2007) Analysis of calculating methods for hobbing force. Tool Eng 03:42–45. https://doi.org/10.16567/j.cnki.1000-7008.2007.03.012

15. Cong F, Chen J, Dong G, Pecht M (2013) Vibration model of rolling element bearings in a rotor-bearing system for fault diagnosis. J Sound Vib 332:2081–2097. https://doi.org/10.1016/j.jsv.2012.11.029

16. Goyal D, Vanraj PBS, Dhami SS (2017) Condition monitoring parameters for fault diagnosis of fixed axis gearbox: a review. Arch Comput Methods Eng 24:543–556. https://doi.org/10.1007/s11831-016-9176-1

17. Althubaiti A, Elasha F, Teixeira JA (2022) Fault diagnosis and health management of bearings in rotating equipment based on vibration analysis – a review. J Vibroeng 24:46–74. https://doi.org/10.21595/jve.2021.22100

18. Cho DW, Choi WC, Lee HY (2000) Detecting tool wear in face milling with different workpiece materials. Key Eng Mater 183–187:559–564. https://doi.org/10.4028/www.scientific.net/KEM.183-187.559